J. Microelectron. Packag. Soc., 29(2), 53-58 (2022) https://doi.org/10.6117/kmeps.2022.29.2.053
Print ISSN 1226-9360 Online ISSN 2287-7525

Resistive Switching Properties of N and F co-doped ZnO

Minjae Kim, Kyung-Mun Kang, Yue Wang, Akendra Singh Chabungbam, Dong-eun Kim, Hyung Nam Kim, and Hyung-Ho Park†

Department of Materials Science and Engineering, Yonsei University, Seoul 03722, Republic of Korea

(Received May 17, 2022: Revised June 23, 2022: Accepted June 30, 2022)

Abstract: One of the most promising emerging technologies for the next generation of nonvolatile memory devices based on resistive switching (RS) is the resistive random-access memory mechanism. To date, RS effects have been found in many transition metal oxides. However, no clear evidence has been reported that ZnO-based resistive transition mechanisms could be associated with strong correlation effects. Here, we investigated N, F-co-doped ZnO (NFZO), which shows bipolar RS. Conducting micro spectroscopic studies on exposed surfaces helps tracking the behavioral change in systematic electronic structural changes during low and high resistance condition of the material. The significant difference in electronic conductivity was observed to attribute to the field-induced oxygen vacancy that causes the metal-insulator Mott transition on the surface. In this study, we showed the strong correlation effects that can be explored and incorporated in the field of multifunctional oxide electrons devices.

Keywords: RRAM, atomic layer deposition, co-doping, oxygen vacancy, Mott-transition

1. Introduction

Comparing the new concepts of non-volatile memory technology among the researchers, such as phase-change Random Access Memory (RAM), magneto-resistive RAM, and ferroelectric RAM, the low operating voltage and simple structure of RAM drew a lot of attention. Resistive Random Access Memory (RRAM) works on structure of metal insulator metal (MIM) and can read and write at a high speed. Thus, it is evaluated as a promising next-generation nonvolatile memory candidate. In the non-volatile memory research area, the material that can control two or more states and maintain them is of paramount importance. Resistance changes caused by electric fields have previously been seen in MIM structures of various transition metal oxide materials with asymmetric electrodes, and these changes have been explained by a number of mechanisms. From this point of view, RRAM has a great advantage of being able to use various characteristics at low cost using various materials and simple structure.[1-8)]

A RRAM composed of an insulating or semiconductor oxide between metal electrodes (MOM structure) which shows a RS occurs in a reversible way when an anode or unipolar voltage is applied. For bipolar RS, application of two voltage polarity leads the device to transition from a high resistance state (HRS) to a low resistance state (LRS). This RS type mechanism is usually used for voltage-driven movement of oxygen ions, pores,[1-4)] changes in barrier such as Schottky by trapping/detrapping effects in interface fault conditions,[5,6)] and Mort transitions.[7,8)] The resistance changes between the metal electrode and the oxide cause by a various mechanism including Schottky, Poole–Frenkel and Fowler–Nordheim.

Erstwhile, the better understanding of the working mechanism for resistive switching in oxides is vital in developing RRAM materials application in neuromorphic devices, but it has not been clearly explained. Interface defects is an important issue in trapping/detrapping type switching mechanisms, which require investigation to understand the phenomenon of insulation or semiconductor oxide structures between metal electrodes. As reported in previous studies, unipolar and bipolar resistance effects conversions were shown in ZnO films. In current research, the resistance of the manufactured device was switched by placing the tungsten tip in direct contact with the Top electrode (TE)-exposed NFZO surface as shown in Fig. 1(a). Following that, it is feasible to conduct a sequential spectroscopic study of difference in electronic structure at the bare

†Corresponding author
E-mail: hhpark@yonsei.ac.kr

surface are possible.[9,10)]

In general, piezoelectric force microscopy (PFM) can be applied to investigate the corresponding polarization switching behavior.[11,12)] For memory applications, the retention and stability of the device is a major issue. Therefore, this study explores the maintenance of RS behavior, possible factors affecting RS retention and relaxation in NFZO thin films, including the electroforming process, scan rate and scan time.

2. Experimental Section

2-1. Materials and deposition condition.

100 nm thick NFZO sample was deposited on TiN/SiO_2/Si substrates at a deposition temperature of 100ºC and operating pressure of ~ 1 Torr using a Lucida D100 system thermal ALD (NCD Technology, Inc. Korea). Precursors for the Zn, O and N reactants were Diethyl zinc (DEZ, EG Chemical Co., Ltd., Korea), deionized water (DI water) and dimmed NH_4OH, respectively. The deionized water (50 mL) and diluted hydrogen chloride (0.5 mL) (33-40% HF diluted in water) were mixed to prepare a homemade F.[13)] The chiller was used to deliver DEZ at less than 10 ºC. As carrier gas, high purity N_2 (99.999%) was used with a flow rate of 20 sccm (standard cubic centimeters per minute). The ALD growth supercycle of NFZO thin film is DEZ pulse (0.1 sec) → N_2 purge (10 sec) → NH_4OH pulse (0.1 sec) → N_2 purge (10 sec) → DEZ pulse (0.1 sec) → N_2 purge (10 sec) → NH_4OH Pulse (0.1 sec) → N_2 purge (10 sec) → DEZ pulse (0.1 sec) → N_2 purge (10 sec) → H_2O/HF pulse (0.1 sec) → N_2 purge (10 sec). The ALD growth cycle was adjusted to produce the desired thin film.

2.2. Characterization of Thin Films

Examining the thickness, phase formation and crystallinity of the NFZO thin films was done by X-ray diffraction analysis (XRD, D / MAX-2000, Rigaku) utilizing Cu Ka radiation and Scanning electron microscopy (SEM, JSM-600F, JEOL) respectively. To measure the RS behavior of NFZO thin films, a two-probe measurement equipment and a semiconductor device analyzer (Agilent B1500A) were used.

The experimental setup is shown in Fig. 1. NFZO films were investigated by using SPEM, O 1s Near X-ray absorption microstructure (NEXAFS), ultraviolet photoelectron spectroscopy (UPS) (He I radiation 21.22 eV) and photoemission spectroscopy in an ultra-high vacuum chamber of the beamline 8A1 at the Pohang Accelerator Laboratory after switching between HRS and LRS regions with tungsten tips in air. To measure the repeatability of these characteristics, we switched from the HRS region to the LRS region after ten sweeps, respectively.

SPEM was measured by focusing a monochromatic x-ray with a Fresnel zone plat. The spatial absorption distribution of a horizontally polarized beam was measured to obtain SPEM images. In SPEM measurements, incident beam with energy 529 eV was used to identify local HRS and LRS regions. The beam flux was about 109 photons s^{-1}, and the SPEM's spatial resolution was about 500 nm × 300 nm. PES and NEXAFS in the detected HRS and LRS regions were measured by focused x-ray beams. Within the switched area, the NEXAFS of the NFZO thin film was measured with polarized photons at normal incidence horizontally. The UPS measurements were taken at a 45º angle of incidence with normal emission to the surface. With CCD cameras and manipulators, the photon beam was smaller than 500 mm in diameter and focused at the switch area.

The local piezoelectric response was investigated by using conductive Pt/Ir-coated Si cantilever tip along with a piezoelectric force microscopy (PFM: Nanoscope V multimode, Bruker). A PFM operating in lock-in mode at 20 kHz with an applied drive voltage of 10 V was used to acquire the PR amplitude distribution over a local surface area of 3 × 3 μm^2. The amplitude values obtained by PFM measurements were adopted to estimate the out-of-plane piezoelectric coefficients d_{33}.

3. Results and Discussion

3.1. Resistive Switching Characteristics

In previous research demonstrated there was no RS properties in just the ZnO.[14)] In addition, previous research suggested NFZO favored the production of p-type ZnO because fluorine can delocalize N acceptor states and provide shallower acceptor levels in ZnO.[15,16)] Fluorine is especially appealing because it can passivate V_o in addition to being a donor dopant for ZnO.[17)] Consequently, we respectively used N and F as the acceptor and donor to generate the acceptor-donor complex for the production of p-type ZnO.[14)] The I–V characteristics of NFZO shown in Fig. 2(a) present the effect of RS due to swift set and reset process. To The resistance changes was observed at voltages of +5.9 V and -5.4 V, respectively. In Fig. 2(a), the initial state is changed from HRS to LRS by positive bias. If a negative bias is applied after the LRS transition, it starts at HRS and switches back to LRS. The function of oxygen vacancies may induce a change in the height and/or width of the barrier or help controlling the carrier concen-

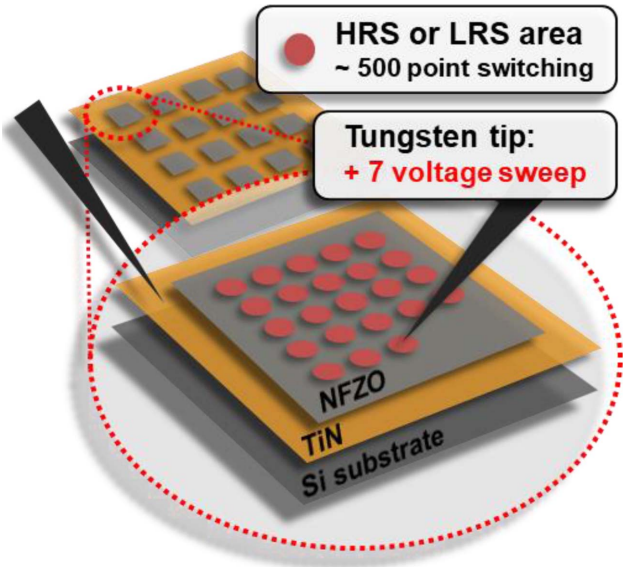

Fig. 1. Scheme of sample preparation for measurement. The resistive switching measured using W tip (5 mm tip diameter).

tration.[18,19] In p-type oxide semiconductors, for example, oxygen vacancies are considered acceptor scavengers. Therefore, oxygen vacancy concentration decrease at the interface under a positive bias field narrows the depletion region in the NFZO, which leads to reduction in contact resistance, resulting in counter-clockwise I-V characteristics.

To understand the switching mechanism in NFZO, the I-V curve for positive forward bias region was plotted at the log-log scale as follows (Fig. 2(b)). The HRS conduction mechanism shows $I \propto V$ correlated to ohmic conduction under the low electric field, subsequently $I \propto V^3$, which may be due to a space charge limited conduction (SCLC) mechanism corresponding to the nonuniform energy or spatial distribution of electron traps.[20] Since SCL conduction is related to trap located at the ZnO interface and a primary operating mechanism that does not induce changes at the interface region, which is recommended due to limited conduction such as bulk at the interface. Resistive switching of ZnO thin films has been reported to be associated with oxygen deficiency.[21,22]

HRS is well described by the SCL conduction mechanism, which suggests a change in the Schottky-type barrier region from defects localized by electron charge/discharge to the surface area along with hysteresis behavior. Normally, traditional single-carrier injection SCL trap controlled conduction was not considered trapped carrier retention behavior after bias removal and the significant rise in current when transitioning from LRS to HRS. As a result, in this work, the interface Mott transition switching

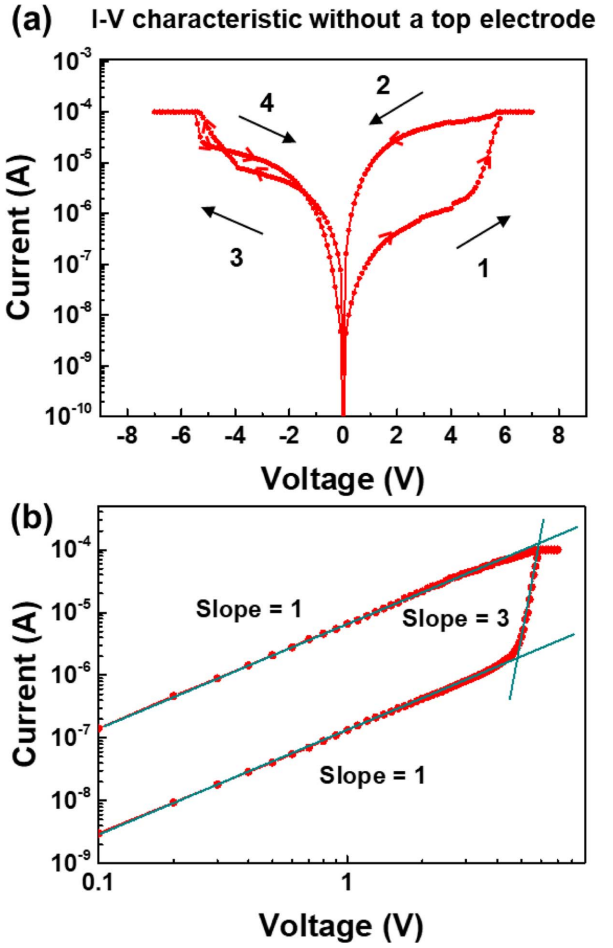

Fig. 2. (a) Resistive switching for W-probe/NFZO/TiN under 0 → +7 → 0 → -7 → 0 V DC voltage sweep, (b) The log-log I-V curve of NFZO device in the positive-voltage region.

mechanism was investigated. Metal-insulator transitions are exceedingly intricate processes, and a variety of operating mechanisms, including electron correlation, defect trapping/de-trapping, and combinations thereof, can occur in RRAM devices. In this case, metal and insulating states can coexist, and the device's I-V characteristics show high nonlinearity and memory effects.

Chan et al. reports the band structure analysis that II-VI semiconductors has cationic vacancies demonstrated mott-insulation behavior in Zn compounds and show the possibility of ferromagnetic interactions between local spins among the vicinity of zinc vacancies V_{Zn}. This V_{Zn} presented in the ZnO acts as a trap for interface switching area and has a vital role on carrier transmission. During HRS, the trap center was devoid and ready to seize the charged carrier. When negative forward voltage was applied, electrons were trapped by V_{Zn} and/or clusters, causing the interface area to change into the metal state and the NFZO to be converted to LRS.

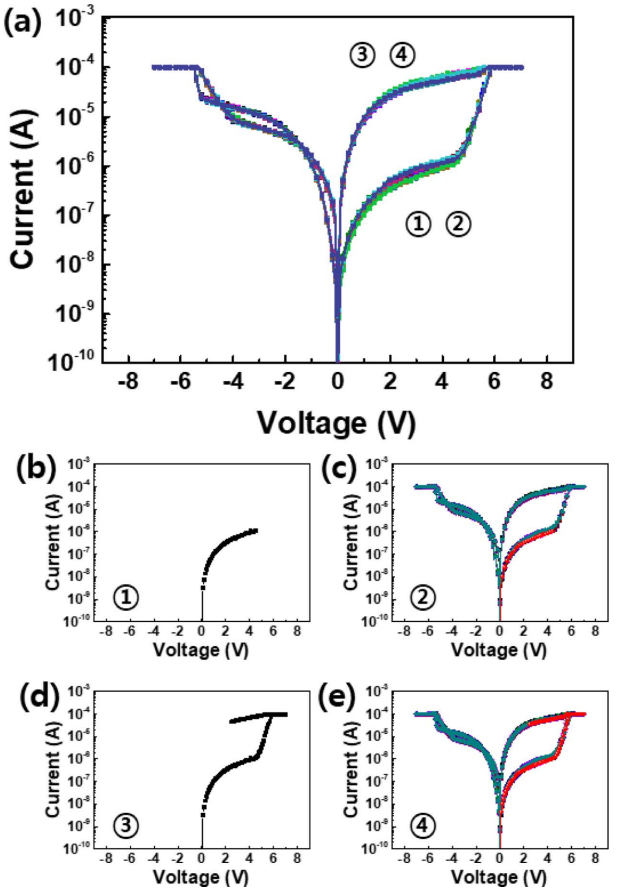

Fig. 3. (a) Resistive switching for W-probe/NFZO/TiN under 0 → +7 → 0 →-7 → 0 V voltage sweep; (b) Initial I-V curve in HRS, (c) I-V curve in HRS after 10 resistive switching cycle, (d) Initial I-V curve in LRS, (e) I-V curve in LRS after 10 resistive switching cycle.

3.2. SPEM and UPS Analysis of N, F Co-doped ZnO

The RS phenomenon is widely documented to be spatially non-uniform. As a result, an experiment was carried out to investigate the geographical distribution of the RS area on the sample surface in order to answer the prior issue. Scanning photoelectron microscopy (SPEM) studies were performed with in the locally switched area after switching to HRS or LRS exploiting tungsten tips individually on the sample surface as shown in Fig. 1. The SPEM studies of samples switched after 10 cycles in the HRS and LRS regions was presented in Fig. 3(a).

Fig. 4 shows SPEM images from O 1s photoemission spectroscopy (PES) on NFZO sample surface depending on the RS cycle. The dark areas in Fig. 4(a, b) represent the HRS region, and the bright areas in Fig. 4(c, d) the LRS region. The spatial absorption distribution of a horizontally polarized beam was measured to obtain SPEM images. The incoming beam's energy was adjusted at 529 eV in SPEM experiments to produce a distribution map of the HRS and LRS areas. The spatial resolution of SPEM was

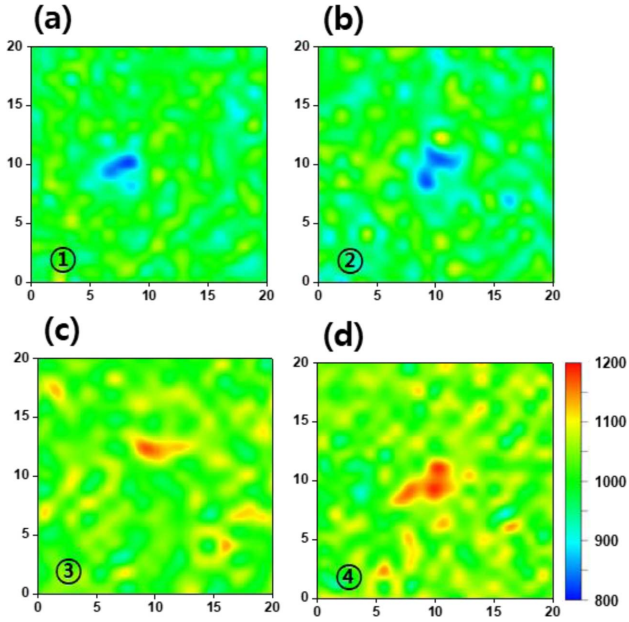

Fig. 4. Scanning photoemission microscopy (SPEM) for O 1s on NFZO film surface within the resistive switching pattern, image size = 20 × 20 um; (a) Initial SPEM image in HRS, (b) SPEM image in HRS after 10 resistive switching cycle, (c) Initial SPEM image in LRS, (d) SPEM image in LRS after 10 resistive switching cycle.

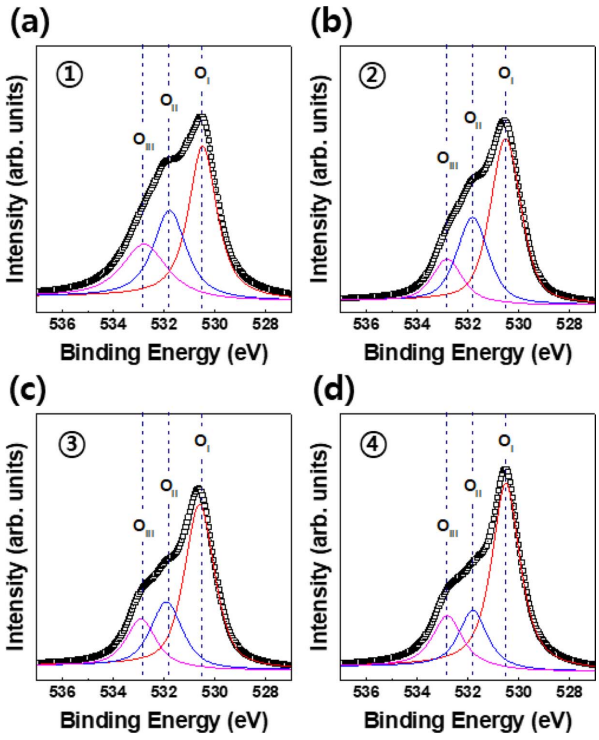

Fig. 5. Deconvolution of PES O 1s spectra with a micro beam; (a) Initial O 1s spectra in HRS, (b) O 1s spectra HRS after 10 resistive switching cycle, (c) Initial O 1s spectra in LRS, (d) O 1s spectra LRS after 10 resistive switching cycle.

about 500 nm × 300 nm. Dark areas with an detected size of about 2 to 5 μm show HRS, which should relate to

increased oxygen deficiency concentrations.

The complete spectrum of O 1s PES taken with a tiny beam inside the dark area (HRS) and inside the bright region (LRS) is shown in Fig. 5. As expected, the spectrum determined within the dark and light areas could be seen to reduce oxygen vacancy for LRS versus HRS. This is expected to be due to a redox reaction between the tungsten tip and NFZO.

Fig. 6(a) shows the ultraviolet photoelectron spectroscopy (UPS) of the NFZO thin film in LRS and HRS states. When binding energy (BE) of ~10.3 eV, it began at the Zn 3d level, and BE < 9 eV was attributed to the O 2p occupied state. The O 2p function at nearly BE 8 eV includes mostly of the O 2p bonded state that hybridizes with the Zn 4s orbit, whereas the function near the valence band (VB) edge (~3 eV) consists primarily of the non-bonding O 2p state. BE in the O 2p state at the VB edge (~3 eV) exhibited a minor change by the same quantity + 0.1 eV in the LRS state. This change appears as a decrease in oxygen vacancies as it changes from HRS to LRS. Fig. 6 (b) shows the Near edge X-ray absorption fine structure (NEXAFS) of the NFZO thin film in LRS and HRS states. According to the results of O 1s NEXAFS analysis in region 1, absorption is observed in the edge part of the LRS state region compared to the HRS region. This is anticipated to be related to reduction producing a defect condition in the conduction band. The energy region 2 is mainly due to the O 2p hybridization with the Zn 3d states located at the bottom of the conduction band.

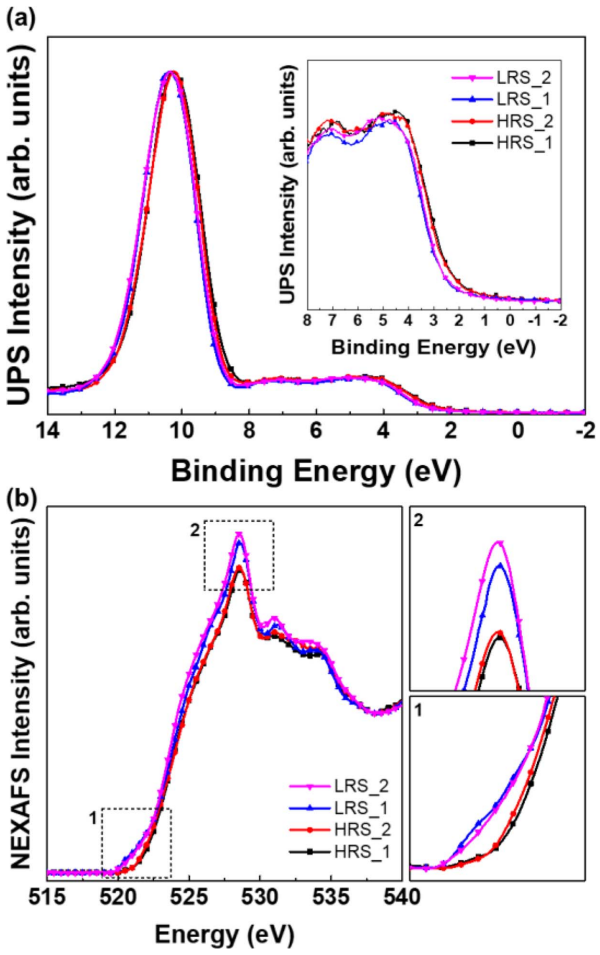

Fig. 6. (a) Ultraviolet photoelectron spectroscopy (UPS) of the NFZO thin film in LRS and HRS states, (b) the X-ray absorption fine structure (NEXAFS) of the NFZO thin film in LRS and HRS states.

It is known that N, F tends to occupy vacant oxygen sites and decrease oxygen vacancies in ZnO and this can also be explained by the piezoelectric analysis of these films. To confirm this, we examined the piezoelectric behavior of the pristine and doped samples and PFM microscopy has been used. Fig. 7(a) shows an increased in piezoelectric response seen which could be due to the substitution of O with N and F atoms in the host lattice could lead to lattice distortion that arises from Zn-O bond changes and improved local electric field after doping.[23] Moreover, similar results are also observed by Wang et al. that the increase in oxygen vacancies leads to decrease in piezoelectric potential.[24] Both samples exhibit 180° phase difference which supports

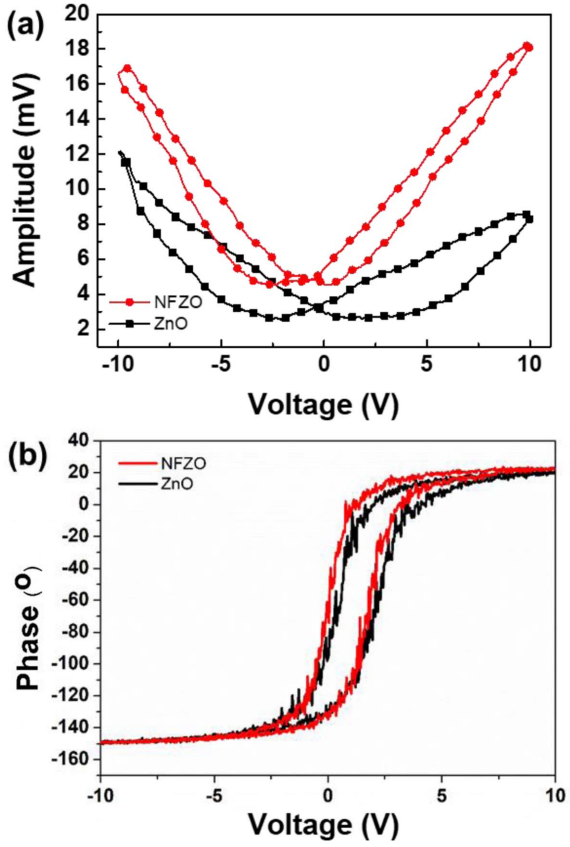

Fig. 7. (a) Piezoelectric response and (b) Phase hysteresis loop under applied electric field of pure ZnO and NFZO measured by PFM.

good attributes of a reversible electric polarization shown in phase hysteresis loop of Fig. 7(b). These types of characteristics observed in NFZO could be helpful in developing new kinds of piezoelectronics and ferroelectric nonvolatile memory device applications.

4. Conclusion

Spectroscopic studies performed directly on the surface of the NFZO proved a strong correlation to the resistive transition of these compounds. Our data analysis reveals that the transition is due to the electric field-induced doping control of the mott insulator. It is critical to highlight that our doping process is similar to one that utilized in low-temperature electrostatic doping in thin film transistors with transition metal oxide channels. The doping accomplished here is nonvolatile and reversible at room temperature.

Acknowledgments

This material is based upon work supported by the National Research Foundation of Korea funded by the Korea government (MSIT) (grant 2019R1A2C2087604). Experiments at PLS were supported in part by MEST and POSTECH.

References

1. R. Waser, R. Dittmann, G. Staikov, K. Szot, “Redox-Based Resistive Switching Memories – Nanoionic Mechanisms, Prospects, and Challenges”, Advanced Materials, 21(25-26), 2632-2663 (2009).
2. A. Sawa, “Resistive Switching in Transition Metal Oxides”, Materialstoday, 11(6), 28-36 (2008).
3. M. J. Rozenberg, I. H. Inoue, M. J. Sanchez, “Nonvolatile Memory with Multilevel Switching: A Basic Model”, Phys. Rev. Lett., 92(17), 178302 (2004).
4. A. Odagawa, H. Sato, I. H. Inoue, H. Akoh, M. Kawasaki, Y. Tokura, T. Kanno, H. Adachi, “Colossal Electroresistance of a $Pr_{0.7}Ca_{0.3}MnO_3$ Thin Film at Room Temperature”, Phy. Rev. B, 70(22), 224403 (2004).
5. A. Sawa, T. Fujii, M. Kawasaki, Y. Tokura, “Hysteretic Current-voltage Characteristics and Resistance Switching at a Rectifying $Ti/Pr_{0.7}Ca_{0.3}MnO_3$ Interface”, Appl. Phys. Lett., 85(18), 4073 (2004).
6. T. Oka, N. Nagaosa, “Interfaces of Correlated Electron Systems: Proposed Mechanism for Colossal Electroresistance”, Phy. Rev. Lett., 95(26-31), 266403 (2005).
7. K. Szot, W. Speier, G. Bihlmayer, R. Waser, “Switching the Electrical Resistance of Individual Dislocations in Single-crystalline $SrTiO_3$”, Nature Materials, 5, 312-320 (2006).
8. Y. B. Nian, J. Strozier, N. J. Wu, X. Chen, A. Ignatiev, “Evidence for an Oxygen Diffusion Model for the Electric Pulse Induced Resistance Change Effect in Transition-Metal Oxides”, Phys. Rev. Lett., 98(14), 146403 (2007).
9. R. Fors, S. I. Khartsev, A. M. Grishin, “Giant Resistance Switching in Metal-insulator-manganite Junctions: Evidence for Mott Transition”, Phys. Rev. B, 71(4), 045305 (2005).
10. M. J. Rozenberg, I. H. Inoue, M. J. Sanchez, “Strong Electron Correlation Effects in Nonvolatile Electronic Memory Devices”, Appl. Phys. Lett., 88(3), 033510 (2006).
11. J. B. Torrance, P. Lacorre, A. I. Nazzal, E. J. Ansaldo, Ch. Niedermayer, “Systematic Study of Insulator-metal Transitions in Perovskites $RNiO_3$ (R=Pr, Nd, Sm, Eu) Due to Closing of Charge-transfer Gap”, Phys. Rev. B, 45(14), 8209 (1992).
12. J. Zaanen, G. A. Sawatzky, and J. W. Allen, “Band Gaps and Electronic Structure of Transition-metal Compounds”, Phys. Rev. Lett., 55(4), 418 (1985).
13. Y. J. Choi, H. H. Park, “A Simple Approach to the Fabrication of Fluorine-doped Zinc Oxide Thin Films by Atomic Layer Deposition at Low Temperatures and an Investigation into the Growth Mode”, Journal of Materials Chemistry C, 2(1), 98-108 (2014)
14. Y. Wang, M. Kim, M. A. Rehman, A. S. Chabungbam, D. E. Kim, H. S. Lee, I. Kymissis, H. H. Park, “Bipolar Resistive Switching in Lanthanum Titanium Oxide and an Increased On/Off Ratio Using an Oxygen-Deficient ZnO Interlayer”, ACS Applied Materials & Interfaces, 14(15), 17682-17690 (2022).
15. H. L. Ju, H. C. Sohn, K. M. Krishnan, “Evidence for O 2p Hole-Driven Conductivity in $La_{1-x}Sr_xMnO_3$ ($0 \le x \le 0.7$) and $La_{0.7}Sr_{0.3}MnO_z$ Thin Films”, Phys. Rev. Lett., 79(17), 3230 (1997).
16. M. Imada, A. Fujimori, Y. Tokura, “Metal-insulator Transitions”, Rev. Mod. Phys., 70(4), 1039 (1998).
17. A. J. Millis, “Lattice Effects in Magnetoresistive Manganese Perovskite”, Nature, 392, 147-150 (1998).
18. S. E. Kim, J. G. Lee, L. Ling, S. E. Liu, H. K. Lim, V. K. Sangwan, M. C. Hersam, H. S. Lee, “Sodium-Doped Titania Self-Rectifying Memristors for Crossbar Array Neuromorphic Architectures”, Advanced Materials, 34(6), 2106913 (2022).
19. S. Hong, T. Choi, J. H. Jeon, Y. Kim, H. Lee, H. Y. Joo, I. Hwang, J. S. Kim, S. O. Kang, S. V. Kalinin, B. H. Park, “Large Resistive Switching in Ferroelectric $BiFeO_3$ Nano-Island Based Switchable Diodes”, Advanced Materials, 25 (16), 2339-2343 (2013).
20. Ch. Jooss, L. Wu, T. Beetz, R. F. Klie, M. Beleggia, M. A. Schofield, S. Schramm, J. Hoffmann, Y. Zhu, “Polaron Melting and Ordering as Key Mechanisms for Colossal Resistance Effects in Manganites”, PNAS, 104(34), 13597-13602 (2007).
21. J. Lee, H. Choi, D. Seong, J. Yoon, J. Park, S. Jung, W. Lee, M. Chang, C. Cho, H. Hwang, “The Impact of Al Interfacial Layer on Resistive Switching of $La_{0.7}Sr_{0.3}MnO_3$ for Reliable ReRAM Applications”, Microelectronic Engineering, 86(7-9), 1933-1935 (2009).
22. S. Q. Liu, N. J. Wu, A. Ignatiev, “Electric-pulse-induced Reversible Resistance Change Effect in Magnetoresistive Films”, Appl. Phys. Lett. 76(19), 2749 (2000).
23. K. Ayeb, N. Moussa, M. F. Nsib, S. G. Leonardi, G. Neri, “NO_2 Sensing Properties of N-, F-and NF Co-doped ZnO Nanoparticles”, Materials Science and Engineering: B, 263, 114870 (2021).
24. P. Wang, X. Li, S. Fan, X. Chen, M. Qin, D. Long, M. O. Tadé, S. Liu, “Impact of Oxygen Vacancy on Piezo-catalytic Activity of $BaTiO_3$ Nanobelt”, Applied Catalysis B: Environmental, 279, 119340 (2020).